

MAGNETIC MODELING OF THE SUBSURFACE STRUCTURE OF SHIP ROCK, NEW MEXICO

ANDISHEH BEIKI

University of Toronto

Research Advisor: Dr. Charly Bank

INTRODUCTION

Ship Rock is a prominent volcanic neck of the Navajo Volcanic Field. The diatreme, mainly made of tuff breccia and minnette, is believed to be the result of a maar-type eruption (Semken, 2003). There are seven visible dikes radiating from the diatreme, the largest one being up to 30 m high, 2m wide, and approximately 8 km long.

So far, only visible attributes have been utilized to deduce theories regarding the magmatism and structural processes which led to the formation of Ship Rock. Delaney and Pollard (1981) propose a temporal sequence of events, beginning with dike emplacement, followed by channeling of magma through the diatreme and plugs that grow by erosion of the host rock. They discuss mechanical models of dike dilation and propagation, as well as models of magma flow and heat loss during dike emplacement. However, such models and hypotheses cannot be substantiated without an appropriate model of the subsurface structure. To learn more about the subsurface of Ship Rock, we conducted a magnetic survey of the area. We investigate whether the dikes connect and merge in the subsurface and whether the plugs near the diatreme are related to these subsurface dikes. For the 3 major dikes (South, West, and Northeast) we examine the shape and dip of the dikes near the ends and determine their depth and thickness at various locations. We compare our results to models of magma emplacement proposed by Delaney and Pollard (1981).

GEOPHYSICS BACKGROUND

The magnetic method is employed to find anomalies caused by contrasts in magnetization or magnetic susceptibility. The igneous rocks present at Ship Rock can be expected to have a high magnetic susceptibility (6×10^{-2}) compared to the host rock, Mancos Shale (7×10^{-4} ; Telford, 1990). Rocks of higher magnetic susceptibility will acquire a stronger induced magnetization under the influence of the geomagnetic field; therefore dikes and other igneous intrusions are easily distinguishable by the magnetic anomaly they cause. For simple bodies, the wavelength of the anomaly contains information regarding the depth and shape of the anomaly. Deeper structures result in large wavelength anomalies, while shallow structures result in smaller wavelength anomalies (Sharma, 1997). The shape of the magnetic anomaly changes with the inclination of the earth's field and also depends on the shape of the source body and its direction of magnetization. Therefore, the anomaly caused by a dike, approximated by a relatively thin vertical slab, will be different from the anomaly caused by a spherical body (Sharma, 1997). This allows us to differentiate between the structures causing the anomalies and thus makes the magnetic method quite ideal for the intentions of this project.

Magnetic data requires processing in order to obtain maps and models of subsurface structures. Processing steps may include diurnal corrections, reduction-to-pole, 2D/3D forward modeling, analytical signal calculation, upward

continuation, and inverse modeling. Processing allows us to limit our data to the magnetic field of the geologic structure and uninfluenced by any external factors, such as the earth's field and surrounding metal objects (Sharma, 1997). For this investigation, we carried out the diurnal correction and proceeded with forward modeling. The diurnal correction is required to account for the temporal variation of the geomagnetic field. This variation is mainly due to electromagnetic radiation from the sun, which causes changes in the strength and direction of currents flowing through the Earth's ionosphere (Burger, 1992). To correct for diurnal variations, we set up a base magnetometer at a predetermined location, allowed it to take measurements at fixed sampling intervals, and subtracted those readings from the readings of our rover magnetometers (Sharma, 1997). Forward modeling is used to generate a theoretical anomaly that is best matched to the measured anomaly (Sharma, 1997). The process requires multiple steps, where the source body characteristics undergo several modifications in order to match the computed with the observed anomaly. The result is a physical model of the geologic structure producing the magnetic anomaly.

DATA ACQUISITION

A total of about 65,000 data points were collected during 13 days of fieldwork. We covered an area of approximately 1,570,000 square meters around Ship Rock (see Fig. 2 in Bank et al., this volume).

We used two GEM-Systems GSM 19-G Overhauser proton-precession magnetometers (PPMs). These rover magnetometers were set on the "walkmag" option, which allows the surveyor to walk continuously while the instrument takes measurements of the total field in two-second time intervals. The base magnetometer, a Geometrics G-856 PPM, collected total field data in sixty-second

intervals to be used for the diurnal correction. The survey was carried out using a modified grid system, where the magnetic lines crisscrossed one another. The magnetometers were carried on-person and the surveyor carrying the instrument also carried a hand-held Global Positioning System receiver (Trimble Navigator Geoexplorer) to track the position of the magnetometer using the NAD83 datum in UTM coordinates.

Error in GPS locations and magnetic field values were the main types of error involved in our measurements. The accuracy of the GPS data was improved from 5 m to 1 m by recording signals from WAAS, a geostationary satellite that broadcasts corrected data. In addition to GPS instrumental error, synchronization error of clocks between the rover magnetometers and the GPS was corrected for by lining up the distinct anomalies resulting from dikes. The magnetic field values were subject to error from both the magnetometer and the GPS receiver. The PPMs had an accuracy of ± 0.1 nT. But interference from metal components in the GPS receiver introduced an additional error of approximately ± 9 nT to the magnetic measurement.

When using geophysical methods, there are always limitations to consider. In the case of the magnetic method, we are limited by a number of factors. First, the measurements are subject to error. Second, the computer codes used to model the data make simplifying assumptions, which reduce the precision to which our data can be modeled. Third, the solution of the magnetic potential function is non-unique. Therefore, determining the shape of the structures in question requires boundary conditions that limit the number of solutions that apply to our problem (Sharma, 1997).

RESULTS AND

INTERPRETATION

During fieldwork, surveyors crossed over areas that were measured on previous days in order to compare magnetic measurements for quality. Figure 1 demonstrates this overlap of magnetic lines. Note that the largest magnetic anomalies are produced by the diatreme and the plugs themselves; in addition rocks broken off from the diatreme cause large localized anomalies which may also mask anomalies produced by the subsurface dikes. Therefore, we could not determine whether or not the dikes merge in the subsurface.

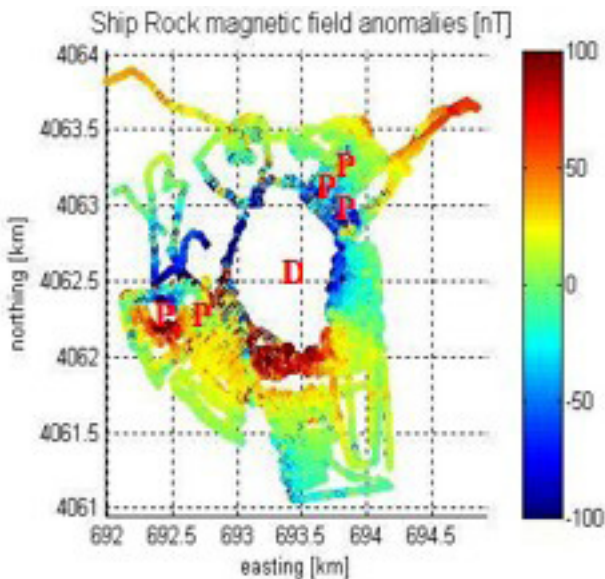


Figure 1. Magnetic field anomalies measured around the diatreme (D) and plugs (P). Note the overlap of magnetic readings on separated days and the large anomalies obtained near the base of the diatreme.

Figure 2(i) is an interpolated graph of magnetic field anomalies in the region between two of the northeastern plugs. We used a forward modeling algorithm by Singh (2002) to produce theoretical magnetic anomalies resulting from an infinitely long 2-D body with arbitrary polygonal cross-section, but uniform volume density and magnetization. Figure 2(ii) and 2(iii) show the anomalies and model along the specified profile respectively, which predict the presence of a subsurface dike linking the plugs and most likely giving rise to the plugs. The model also predicts a smaller vertical dike,

which is most likely a branch off the larger dipping dike. The positioning of the dikes is in agreement with models proposed by Delaney and Pollard (1981), who explain plugs as buds off the dikes.

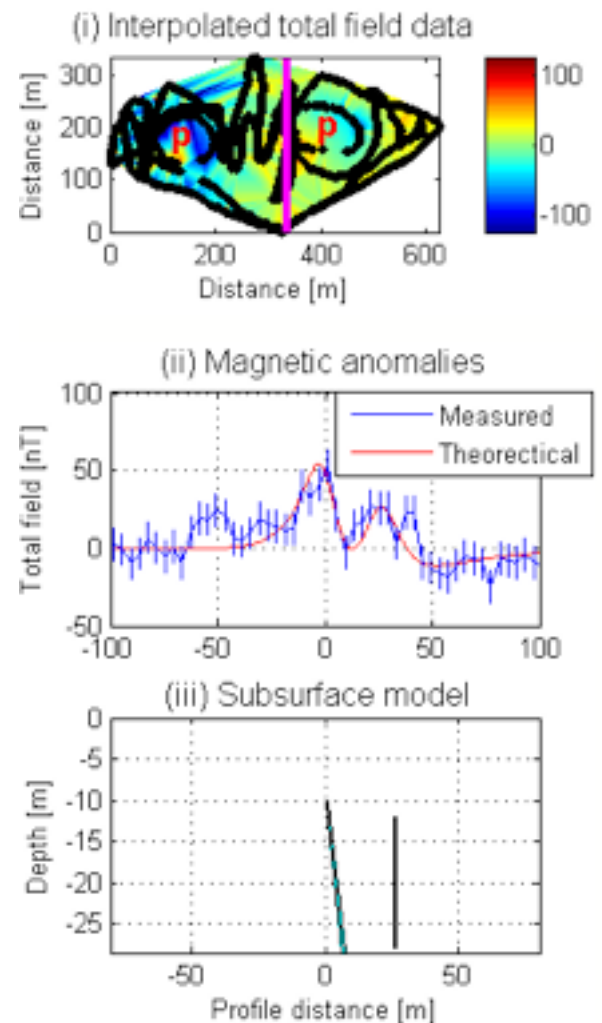


Figure 2. Region between two of the northeastern plugs. (i) Interpolated total field values; pink line represents location of the model profile. (ii) Theoretical anomaly overlain on measured anomaly. (iii) Model of the dikes producing the theoretical anomaly.

Surveys were carried out at the ends of the three major dikes in order to determine how far they each extend underground and whether there is any change in shape or thickness of the dikes near the ends. Models were produced using Singh's (2002) algorithm. For each dike, certain modeling parameters were kept constant

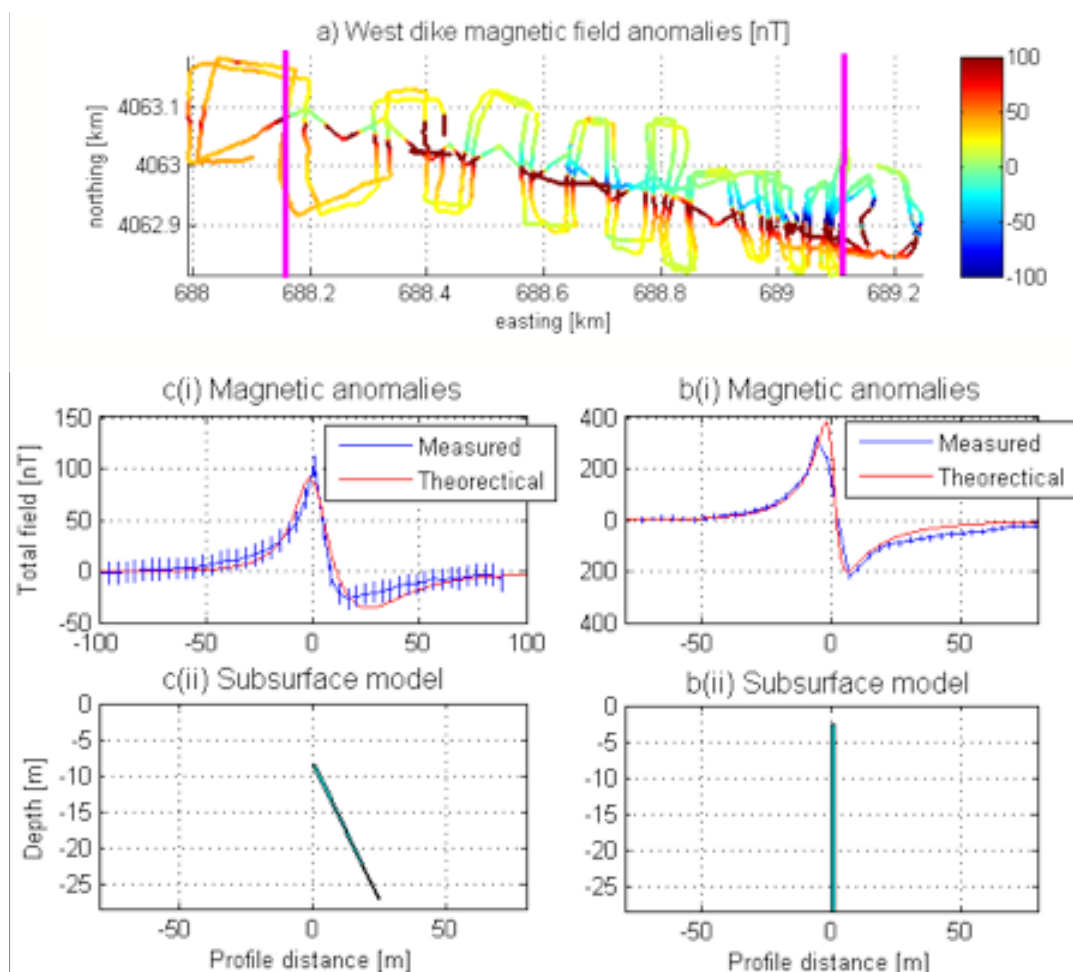


Figure 3. (Left) Magnetic field anomalies (in nT) at the end of the west dike (a). The dike itself is not visible at the surface west of UTM-Easting 689 km. The anomalies b(i) and c(i) correspond to profiles at approximately 689.1 km and 688.15 km easting. The corresponding models b(ii) and c(ii) demonstrate a change in depth, height, thickness, and dip of the dike as we move along its strike.

while others were permitted to vary. The parameters that were permitted to vary include depth, height, and thickness of the source body. Inclination and declination remain constant for the entire survey region. Figure 3(a) is a graph of the total field anomalies measured by our rover magnetometers at the end of the West dike. This dike is not visible at the surface west of 689 km Easting (UTM), but it extends for at least 1 km in the subsurface. We clearly observe a change in magnetic signature along strike of the dike, which portrays a structure with decreasing thickness and increasing depth (Fig. 3(b) and 3(c)). Over a distance of 1 km, the dike progresses 8.5 m into the subsurface and its thickness decreases from 1.3 m (observed at the site of last exposure) to 1.1 m (predicted by forward models).

Figure 4 shows a model of the end of the South dike. The thickness of the dike generally decreases, aside from some local variations. Over the final 3.5 km, the thickness changes from 0.8 m to 0.35 m and the dike proceeds up to 8 m into the subsurface (before rising again at the end). In the surface, we observe a variation in depth of the dike near the end. Models show that this pattern continues until the dike ends. In addition, the models demonstrate a section of the dike to branch off at about 900 m before termination.

CONCLUSIONS

We collected magnetic data over 1,570,000 square meters around Ship Rock. We decided to concentrate on the region between the

northeastern plugs and the ends of the three

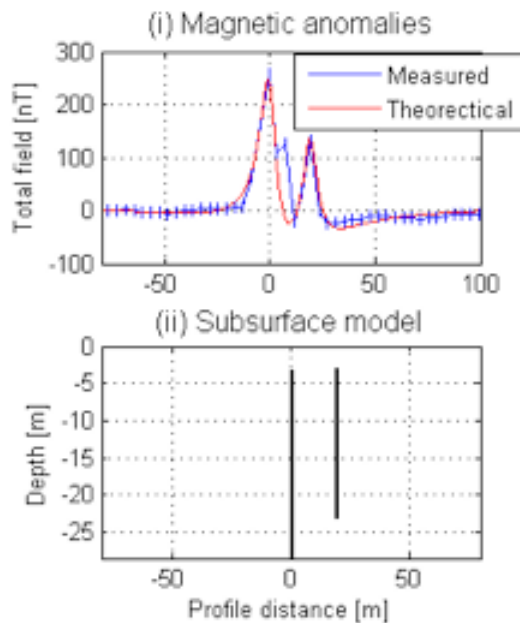


Figure 4. (Above) Model produced for the South dike for a profile at 695.7 km UTM-easting and 4054.3 km UTM-northing. (i) Theoretical anomaly overlain on the measured anomaly. (ii) Model of the section of the dike producing the theoretical anomaly.

major dikes for detailed analysis. The data demonstrates the West dike to propagate underground past its field exposure for over 1 km, the Northeast dike for 0.55 km, while the South dike terminates at the site of its last exposure. We created 2D models of these dikes at several locations, which demonstrate a general pattern of decreasing thickness and increasing depth as we approach the end. Models created for the end of the South dike show it to branch off or segment near the ends. Both the West and South dike have a bottom at approximately 30 m below the surface, while the Northeastern dike has a bottom at approximately 18 m depth. In regards to the northeastern plugs, we propose that a dike connects two of these plugs and most likely gives rise to them. However, we were unable to draw a conclusion regarding the mergence of the dikes in the subsurface. The area close to the diatreme is scattered with large basaltic rocks that create sharp surface anomalies, which could mask any anomaly from deeper structures. In conclusion, our interpretations are in agreement with models of dike flow and plug

formation proposed by Delaney and Pollard (1981). Further investigation would require 3D modeling of our data set to gain an even better understanding of the subsurface structure of Ship Rock.

ACKNOWLEDGEMENTS

Field work on the Navajo Nation was conducted under a permit from the Navajo Nation Minerals Department, and persons wishing to conduct geologic investigations on the Navajo Nation must first apply for, and receive, a permit from the Navajo Nation Minerals Department, P.O.Box 1910, Window Rock, Arizona 88515, telephone (928) 871-6587.

REFERENCES

- Burger, H. R., 1992, Exploration geophysics of the shallow subsurface. 489 pages, Prentice-Hall, Upper Saddle River, USA.
- Delaney, P.T., and D. D. Pollard, 1981, Deformation of host rocks and flow of magma during growth of minette dikes and breccia-bearing intrusions near Ship Rock, New Mexico: U.S. geological Survey Professional Paper 1202, 61 p.
- Semken, S.C., 2003, Black rocks protruding up: the Navajo Volcanic Field, New Mexico Geological Society Guidebook, p.133-138.
- Sharma, P. V., 1997, Environmental and engineering geophysics, 475 pages, Cambridge University Press, Cambridge, UK.
- Singh, B., 2002, Simultaneous computation of gravity and magnetic anomalies resulting from a 2-D object, *Geophysics*. Vol. 67, No. 3; p.801-806.
- Telford, W. M., L. P. Geldart, and R. E. Sheriff, 1990. *Applied Geophysics*, 2nd edition, 770 pg., Cambridge University Press, Cambridge, UK.